Aerosol and Air Quality Research

ORIGINAL RESEARCH
https://doi.org/10.4209/aaqr.220361

Vertical Characteristics of Potential $PM_{2.5}$ Sources in the Urban Environment

Ho-Tang Liao [1†], Yu-Chi Lai [1†], Hsing Jasmine Chao [2], Chang-Fu Wu [1,3*]

[1] Institute of Environmental and Occupational Health Sciences, College of Public Health, National Taiwan University, Taipei 10055, Taiwan
[2] School of Public Health, College of Public Health, Taipei Medical University, Taipei 11031, Taiwan
[3] Department of Public Health, College of Public Health, National Taiwan University, Taipei 10055, Taiwan

Special Issue:
2022 Asian Aerosol Conference (AAC 2022) (III)

ABSTRACT

Exposure to urban air pollution, particularly fine particulate matter ($PM_{2.5}$), is known to be harmful to human health. Source apportionment of urban $PM_{2.5}$ provides information to develop effective control strategies, thus reducing the exposure concentrations and health risks. However, this is a challenging task in metropolitan areas where people live in high-rise buildings. To understand the vertical characteristics of air pollution sources in urban areas, a total of 114 vertically stratified $PM_{2.5}$ samples were collected at six heights (1st, 7th, 10th, 13th, 17th, and 20th floors) of one building during the period between 19 October and 22 December 2020. Absorbance, 16 trace elements, 8 water-soluble ions, and water-soluble organic carbon on Teflon-membrane filters were measured. Positive Matrix Factorization was utilized to achieve the source apportionment analysis. Six source factors, including biomass burning/industry, traffic related, secondary aerosol, soil dust, contaminated road dust, and sea salt, were retrieved. During the sampling period, the major contributor to $PM_{2.5}$ was secondary aerosol (28.8%), followed by biomass burning/industry (24.4%) and traffic related (13.3%). It should be noted that road traffic emissions (traffic related and contaminated road dust) accounted for 24.7%, making them the second largest contributor to $PM_{2.5}$. Contributions of road traffic emissions significantly declined with height (29.3%–21.4%), which was in line with the findings in previous studies, and could explain the vertical variation of $PM_{2.5}$ identified in this study. These findings help estimate the realistic exposure at different residential heights, consequently facilitating control strategy development.

Keywords: Source apportionment, Fine particulate matter, Positive matrix factorization, Water soluble organic carbon, Vertical distribution

OPEN ACCESS

Received: October 25, 2022
Revised: December 27, 2022
Accepted: January 3, 2023

* **Corresponding Author:**
changfu@ntu.edu.tw

† These authors contributed equally to this work

Publisher:
Taiwan Association for Aerosol Research
ISSN: 1680-8584 print
ISSN: 2071-1409 online

1 INTRODUCTION

In 2018, the urban population was more than 50% in the world and accounted for 78% in more developed regions, including Taiwan (United Nations, 2018). In addition to many benefits of urban life, rapid urbanization also results in some negative impacts such as poor air quality. Exposure to air pollution has been associated with numerous adverse health effects and caused approximately seven million premature deaths worldwide in 2016 (WHO, 2021). These effects, including cardiopulmonary disease and cancer, were closely associated with fine particulate matter ($PM_{2.5}$) that can penetrate into and be deposited in the lung (Kim *et al.*, 2015; Lu *et al.*, 2015; IARC, 2016). To develop effective control strategies, identifying urban $PM_{2.5}$ sources and quantifying their contributions to the exposure concentrations and health risks are warranted. The multivariate Positive Matrix Factorization (PMF) solution is a useful tool for apportioning sources of $PM_{2.5}$ (Hopke *et al.*, 2020; Schneider *et al.*, 2022; Silva *et al.*, 2022). The source apportionment analysis is carried out by solving the chemical mass balance equation. Given the speciated

concentration data x_{ij} and the measurement uncertainty u_{ij}, PMF simultaneously estimates factor contribution g_{ik} and factor profile f_{kj} during the iterative process to obtain a minimum of objective function Q (Paatero and Tapper, 1994; Hopke, 2016).

The vertical distribution of source contributions is a critical issue in the urban area where people live in high-rise buildings (Zauli Sajani *et al.*, 2018; Chen *et al.*, 2020). To date, only a few source apportionment studies have been conducted focusing on the vertical distribution of contribution estimates of $PM_{2.5}$ sources at different heights (Wu *et al.*, 2015; Wang *et al.*, 2016; Liao *et al.*, 2020, 2021). In addition, there was great variation in the altitudes investigated due to different sampling strategies among studies. For example, two studies were conducted at two or four heights at a 225-m-high meteorological tower (Wu *et al.*, 2015; Wang *et al.*, 2016), which is much higher than the surrounding residential buildings. The other two source apportionment studies in Taiwan collected $PM_{2.5}$ samples at three floors from buildings lower than 40 m and concluded that traffic related emissions showed decreasing trends with increasing height (Liao *et al.*, 2020, 2021). Nonetheless, the proportion of high-rise buildings is getting increased in urban areas. To better understand the vertical variation of urban residential exposure to ambient $PM_{2.5}$, this study was conducted at one building that has more than twenty floors (approximately 70 m) to collect vertically stratified samples at six heights. PMF was applied to the measured $PM_{2.5}$ components to explore the vertical characteristics of $PM_{2.5}$ sources in metropolitan areas, thus providing more information in designing pollution control strategies.

2 METHODS

2.1 Data Collection

In Taiwan, more than three quarters of the population live in urban areas. Taipei metropolis, which has the highest population density in Taiwan and numerous high-rise buildings, was chosen to explore the vertical characteristics of urban $PM_{2.5}$ sources. Vertically stratified samples were simultaneously obtained at six floor-levels (1st, 7th, 10th, 13th, 17th, and 20th floors) of one building that has balconies facing a major road. The sampler inlets were set at approximately 1.5 m, 20.1 m, 30.9 m, 41.7 m, 52.5 m, and 63.3 m above ground level, respectively. Adjacent to the sampling sites is a low building, which is 20 meters away. In addition, another building across from the sampling sites is 40 meters away. Therefore, the street configuration is considered having a minor effect on the environmental conditions of the sampling sites. Ambient $PM_{2.5}$ samples were collected on pre-weighed 37 mm Teflon-membrane filters (Pall Corporation, Ann Arbor, MI, USA) using multiple Harvard Impactors (Air Diagnostics and engineering, Inc., Harrison, ME, USA) on the balconies. The 24-h integrated filter samples (10:30–10:30 local time) were collected twice a week (every Monday and Thursday) during the period between 19 October and 22 December 2020.

The sampled Teflon-membrane filters were re-weighed using a microbalance (UMX2, Mettler-Toledo International Inc., Greifensee, Switzerland) in a temperature- and humidity-controlled chamber (21–25°C and 30–40%), followed by measurements of absorbance using a Smoke Stain Reflectometer (Diffusion System Ltd, London, UK). Concentrations of 16 trace elements (Mg, Al, Si, S, K, Ca, Ti, V, Cr, Mn, Fe, Ni, Cu, Zn, Ba, and Pb) on the filters were quantified using a non-destructive energy-dispersive X-ray fluorescence method (Epsilon 4, Malvern Panalytical Ltd., Almelo, Netherlands). Subsequently, aqueous extracts of the filters were analyzed for water-soluble organic carbon (WSOC) and eight water-soluble inorganic ions (Cl^-, NO_3^-, SO_4^{2-}, Na^+, NH_4^+, K^+, Mg^{2+}, and Ca^{2+}) using a total organic carbon analyzer (Aurora 1030W TOC analyzer, OI Analytical, College Station, TX, USA) and ion chromatography (model DX-120, DIONEX, Sunnyvale, CA, USA), respectively. Lab and field blank samples were collected and analyzed to detect contamination in sample handling. The method detection limit (MDL) was determined as the triple standard deviation calculated from replicate analyses of lab blank samples (elements) or the lowest concentration of the calibration curve (WSOC and ions). In each batch of filter samples one control sample with known amount of certified standards was measured for validation of data quality.

2.2 Data Analysis

The U.S. EPA's PMF program (the latest version 5.0) was utilized to achieve the source apportionment analysis (Norris *et al.*, 2014). As shown in Eq. (1), the iterative run simultaneously estimates factor contribution g_{ik} and factor profile f_{kj} and converges after obtaining the best-fit Q-value (Norris *et al.*, 2014):

$$Q = \sum_{i=1}^{n}\sum_{j=1}^{m}\left(\frac{e_{ij}}{u_{ij}}\right)^2 = \sum_{i=1}^{n}\sum_{j=1}^{m}\left(\frac{x_{ij} - \sum_{k=1}^{p} g_{ik} f_{kj}}{u_{ij}}\right)^2 \quad (1)$$

where n and m represent the number of samples and species, e_{ij} denotes the matrix of residuals between measurements and predicted values, and p is the number of factors.

The measurement uncertainty u_{ij}, which is essential input in the modeling process, was calculated as (Liao *et al.*, 2017):

$$u_{ij} = \sqrt{\left(0.5 \times MDL_j\right)^2 + \left(0.1 \times x_{ij}\right)^2} \quad (2)$$

where MDL_j represents the species-specific method detection limit.

The BDL value ($x_{ij} < MDL_j$) was considered less reliable and thus was set at MDL/2. The corresponding uncertainty was assigned as MDL × 5/6 to down-weight the BDL value. The signal-to-noise ratio (S/N) calculation in the PMF 5.0 software helps evaluate data quality of each species before running the model. Species having S/N smaller than 0.5 were excluded, while those with S/N ranging from 0.5 to 1 were down-weighted. In addition, species containing more than 70% of BDL values were excluded.

The optimal number of factors was estimated by the maximum individual column mean (IM) and the maximum individual column standard deviation (IS) accompanied by the interpretability of the retrieved profiles, which was examined by the mass fractions and explained variations [EV_{kj} in Eq. (3)] of marker species (Lee *et al.*, 1999; Liao *et al.*, 2020):

$$EV_{kj} = \left[1 - \left(\sum_{i=1}^{n} e_{ij}^2 / u_{ij}^2\right) \Big/ \left(\sum_{i=1}^{n} x_{ij}^2 / u_{ij}^2\right)\right] \times f_{kj} \Big/ \sum_{k=1}^{p} f_{kj} \quad (3)$$

To achieve the total mass apportionment, $PM_{2.5}$ mass was specified as the "Total Variable" in the PMF 5.0 software to eliminate the need for the post-hoc regression process (Norris *et al.*, 2014). Subsequently, the uncertainty of the 'Total Variable' was down-weighted to avoid potentially influencing the model results.

The Wilcoxon signed rank test with Bonferroni correction was conducted in the statistical analysis to examine whether the source contribution estimates were different between floor levels. The SAS 9.3 software was used to perform the test and the result with a p-value < 0.05 was proposed statistically significant.

3 RESULTS AND DISCUSSION

3.1 Source Apportionment

A total of 114 samples (6 floors × 19 days) were collected. Among the measured species, Al, Ti, and Ba were excluded due to their poor data quality. In addition, the elements and their corresponding ions (Mg/Mg^{2+}, S/SO_4^{2-}, K/K^+, and Ca/Ca^{2+}) were well correlated ($r > 0.84$). To avoid double counting, the species with lower S/N (Mg, SO_4^{2-}, K^+, and Ca^{2+}) were excluded. Table 1 shows the 20 variables included in the final model. $PM_{2.5}$ mass ranged from 2.06 to 15.73 μg m^{-3}, with an average concentration of 7.47 μg m^{-3}, throughout the study period. WSOC was the most abundant component in $PM_{2.5}$ at all sampling sites, followed by S and NO_3^-. Recently, WSOC has

Table 1. Vertical variation of speciated data used in PMF modeling at different heights (n = 19 for each site).

Species	Mean (SD) concentration (ng m^{-3}, 10^{-5} m^{-1} for absorbance)					
	1st	7th	10th	13th	17th	20th
$PM_{2.5}$ mass	7921 (3898)	7655 (3696)	7498 (3678)	7314 (3511)	7200 (3748)	7227 (3854)
Absorbance (Abs)	0.97 (0.31)	0.87 (0.34)	0.83 (0.33)	0.78 (0.32)	0.76 (0.33)	0.75 (0.34)
Silicon (Si)	98.6 (83.9)	99.4 (86.1)	93.0 (84.5)	92.8 (86.2)	93.0 (83.7)	96.8 (87.3)
Sulfur (S)	474 (294)	482 (302)	481 (300)	478 (302)	477 (295)	491 (309)
Potassium (K)	39.2 (40.4)	41.7 (39.8)	42.7 (41.2)	40.5 (38.6)	40.0 (35.9)	44.5 (38.8)
Calcium (Ca)	54.4 (29.0)	54.3 (26.2)	50.4 (24.4)	49.5 (27.0)	52.4 (26.9)	54.4 (29.0)
Vanadium (V)	0.77 (0.44)	0.81 (0.48)	0.77 (0.50)	0.77 (0.47)	0.77 (0.46)	0.79 (0.51)
Chromium (Cr)	0.75 (0.65)	0.65 (0.66)	0.57 (0.52)	0.51 (0.50)	0.52 (0.49)	0.62 (0.52)
Manganese (Mn)	8.19 (3.63)	7.45 (3.59)	7.13 (3.60)	6.81 (3.42)	6.61 (3.42)	6.72 (3.88)
Iron (Fe)	93.3 (48.8)	85.4 (47.7)	78.4 (43.7)	74.9 (43.9)	72.5 (42.8)	74.2 (46.2)
Nickel (Ni)	1.16 (0.39)	1.32 (0.95)	1.13 (0.51)	1.02 (0.46)	1.22 (0.45)	1.16 (0.51)
Copper (Cu)	2.74 (1.62)	2.46 (1.66)	2.26 (1.52)	2.16 (1.47)	2.15 (1.48)	2.16 (1.44)
Zinc (Zn)	14.9 (11.2)	14.5 (11.1)	14.2 (10.5)	13.6 (9.9)	13.6 (10.1)	14.0 (10.6)
Lead (Pb)	4.81 (2.05)	4.57 (1.93)	4.50 (1.96)	4.73 (1.96)	4.73 (2.17)	4.45 (2.20)
Chloride ion (Cl_ion)	255 (205)	227 (230)	195 (183)	208 (203)	215 (174)	195 (173)
Nitrate ion (NO_3_ion)	439 (314)	403 (251)	401 (264)	360 (226)	375 (245)	374 (261)
Sodium ion (Na_ion)	334 (223)	344 (240)	326 (215)	324 (214)	312 (224)	312 (211)
Ammonium ion (NH_4_ion)	337 (261)	325 (248)	326 (250)	316 (238)	315 (242)	324 (247)
Magnesium ion (Mg_ion)	45.9 (23.2)	46.8 (23.0)	45.7 (22.6)	45.4 (22.8)	45.5 (21.9)	43.9 (22.8)
Water-soluble organic carbon (WSOC)	760 (417)	733 (405)	720 (398)	699 (399)	701 (391)	746 (384)

become a topic of health concern because of its cytotoxicity caused by reactive oxygen species (Daher *et al.*, 2012; Wang *et al.*, 2018; Jin *et al.*, 2020).

To provide sufficient sample size for receptor modeling, the data was pooled across all floors. A previous study has demonstrated that similar source profiles were retrieved using either the individual datasets or the pooled dataset (Xie *et al.*, 2012). Based on the judging criteria that have been mentioned earlier, the 6-factor solution was considered the best-fit result. The six factors are shown in Fig. 1 and interpreted as follows. Factor 1 is identified by the abundance of S, K, NO_3^-, NH_4^+, and WSOC, accompanied by considerable EVs of K, Cr, Zn, and NH_4^+. K is a tracer of biomass burning activities (Cheng *et al.*, 2009; Gugamsetty *et al.*, 2012), whereas S, NO_3^-, and NH_4^+ could be generated from secondary formation of biomass burning emissions (Song *et al.*, 2005; Thepnuan *et al.*, 2019). Cr and Zn could be associated with industrial emissions (Dai *et al.*, 2015; Lane *et al.*, 2020). Factor 2, characterized by Abs, Cu, Zn, and WSOC, is interpreted as traffic related emissions. Absorbance and WSOC, as surrogates of elemental carbon (EC) and organic carbon (OC), are correlated with traffic emissions in the atmosphere (Jin *et al.*, 2016; Qi *et al.*, 2016; Wen *et al.*, 2018). Cu and Zn can be emitted from the abrasion of brakes and tires (Gugamsetty *et al.*, 2012; Pio *et al.*, 2013; Ponco Wardoyo and Dharmawan, 2019). Zn is also found in lubricating oil used in motor vehicles (Huang *et al.*, 1994; Todorović *et al.*, 2020). Factor 3 is identified by both high loadings and high EVs of S and NH_4^+, accompanied by moderate EVs of V, Na^+, and Mg^{2+}. S and NH_4^+ are the major components of secondary aerosol (Yin *et al.*, 2018; Ghosh *et al.*, 2019). V is a known indicator of oil combustion, which is generally from ship emissions after the phase-out of oil boilers in Taipei City (Pandolfi *et al.*, 2011; Hsu *et al.*, 2017; Liao and Wu, 2020). The presence of Na^+ and Mg^{2+} and absence of Cl^- indicated chloride depletion in aged sea salt (Tang *et al.*, 1997; Sudheer *et al.*, 2014; Adachi and Buseck, 2015). Therefore, Factor 3 is characterized as secondary aerosol that could be from local accumulation and regional transport, accompanied by marine and shipping aerosol. Factor 4 is recognized by the enrichment of Si, which is one of the major crustal elements, and could be interpreted as soil dust (Kim *et al.*, 2003; Wimolwattanapun *et al.*, 2011; Gugamsetty *et al.*, 2012). Factor 5 is characterized by the high EV of Mn and moderate EVs of Abs, Fe, Ni, Pb, and Cl^-, which could be emitted from industrial sources. There were few industries but several road construction sites around the sampling building. Therefore, emissions from the construction equipment and road materials are possible sources of these species, which

ORIGINAL RESEARCH
https://doi.org/10.4209/aaqr.220361

can be deposited on the road and easily re-suspended by traffic (Adachi and Tainosho, 2004; Carrero *et al.*, 2013; Zhang *et al.*, 2014). Factor 6 is characterized by high EVs of Cl^-, Na^+, and Mg^{2+}, which are typical markers of sea salt (Taiwo *et al.*, 2014; Carnelos *et al.*, 2019).

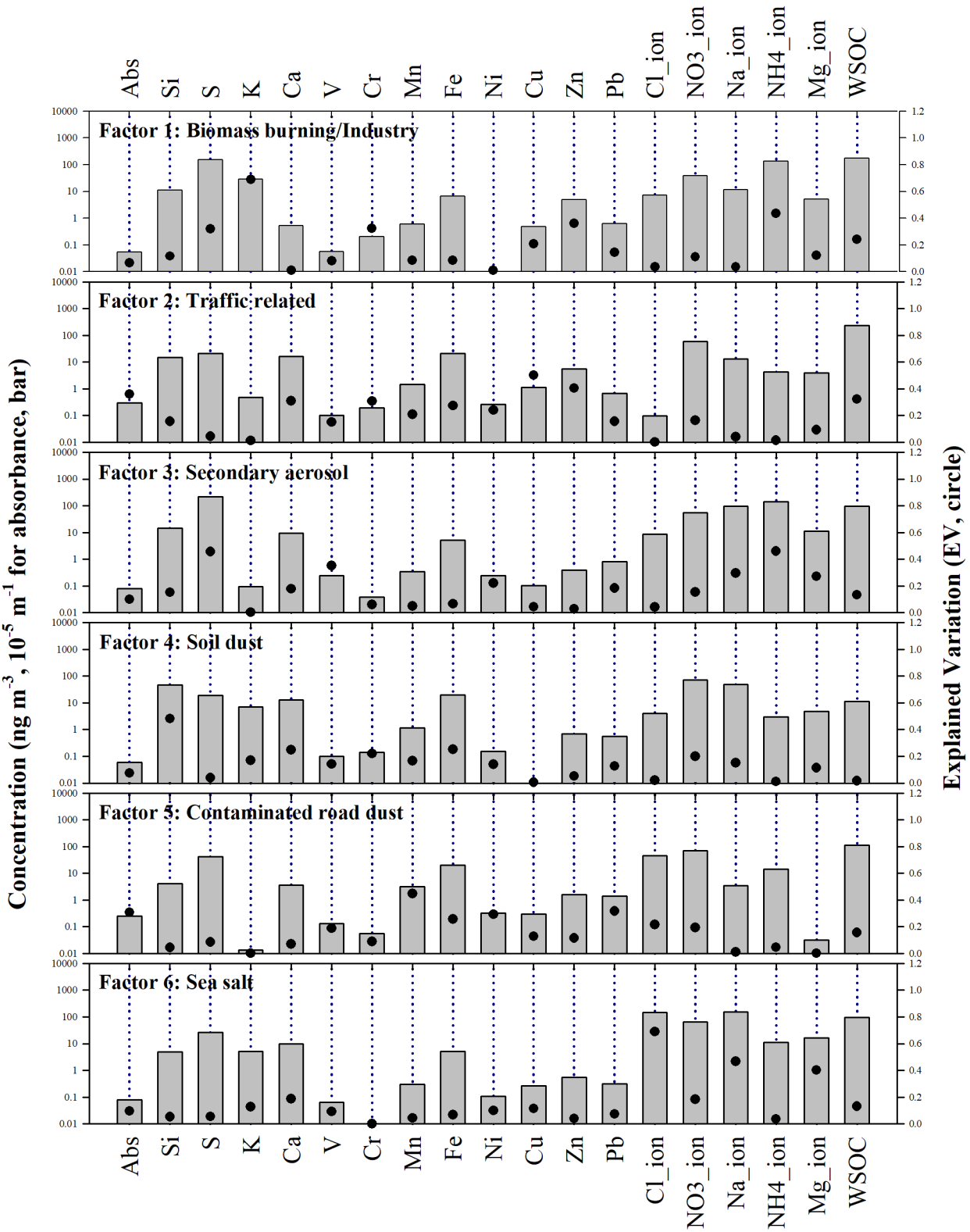

Fig. 1. Factor profiles retrieved from the 6-factor solution of the PMF model run.

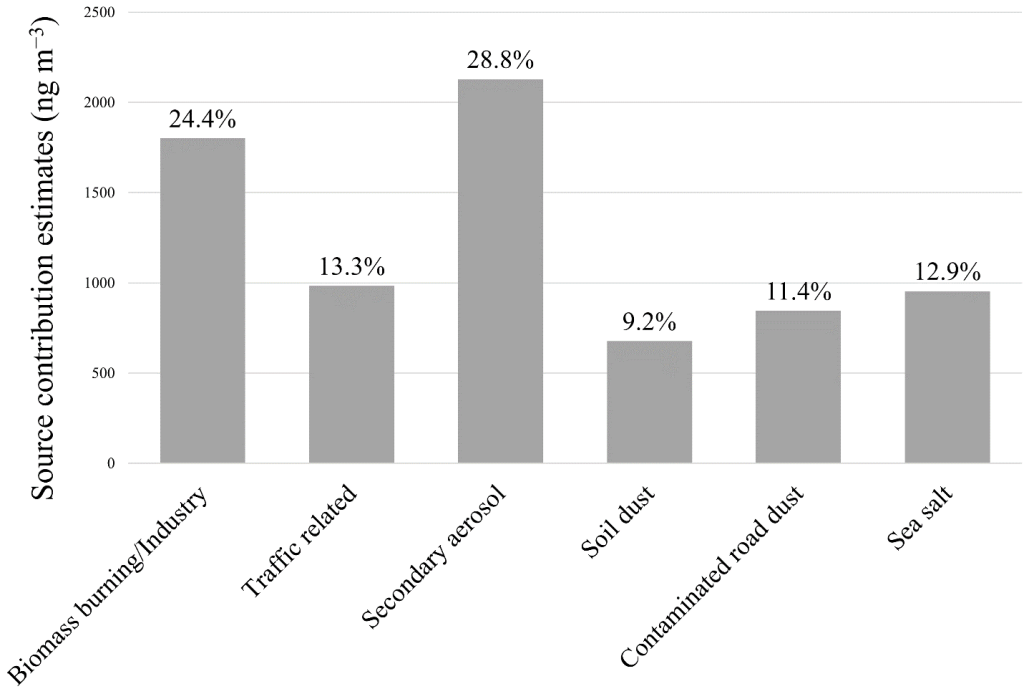

Fig. 2. Source contribution estimates to $PM_{2.5}$ mass at the sampling site during the study period.

As shown in Fig. 2, the major contributor to $PM_{2.5}$ during the sampling period was secondary aerosol (28.8%), followed by biomass burning/industry (24.4%) and traffic related (13.3%) sources. It should be noted that road traffic emissions (traffic related and contaminated road dust) accounted for 24.7%, making them the second largest contributor to $PM_{2.5}$. Above findings were in line with previous studies in Taipei, where secondary aerosol and road traffic accounted for more than half of the contributions to $PM_{2.5}$ (Ho *et al.*, 2018; Liao *et al.*, 2020; Liao and Wu, 2020). With regard to the contributors to WSOC, road traffic emissions accounted for 47.8%, followed by biomass burning/industry (24.0%).

3.2 Vertical Distribution

As shown in Table 1, the vertical distribution patterns were different among variables. Most species, including $PM_{2.5}$ mass, showed the highest concentrations at the two lowest floor levels (1st and 7th), whereas S and K had the greatest concentrations at the 20th floor. Several species, including Si, S, Ca, V, Ni, NH_4^+, Mg^{2+}, and WSOC, showed comparable (difference $<$ 5%) concentrations between the 1st and 20th floors. It should be noted that WSOC exhibited a decreasing trend from the 1st to the 13th floor. The $PM_{2.5}$ mass concentrations generally declined with height, except for that above the 17th floor. $PM_{2.5}$ mass, Abs, Fe, Cu, Zn, and WSOC showed significant differences between lower (1st or 7th) and higher (13th, 17th, or 20th) floor levels. However, no statistically significant difference was found between the 17th and 20th floors. The distribution patterns of $PM_{2.5}$ and traffic-related components, such as Abs (the surrogate of EC) and Fe, were similar to those revealed by Zauli Sajani *et al.* (2018) during the cold season.

Fig. 3 shows the vertical distribution patterns of the source contribution estimates by exhibiting the ratio of contribution at each floor to that at the 1st floor. The significant differences in source contribution estimates between floor-levels were found for traffic related and contaminated road dust. In general, traffic related contributions declined with height, showing significant differences between lower (1st or 7th) and higher (13th, 17th, or 20th) floor levels. Although the contribution at the 20th floor was slightly higher than that at the 17th floor, no statistically significant difference was found between these two floors. Regarding the decreasing trend for the contributions from contaminated road dust, statistically significant difference was found between the 1st and 20th floors, potentially supporting that this factor was likely from local emissions. In contrast, secondary

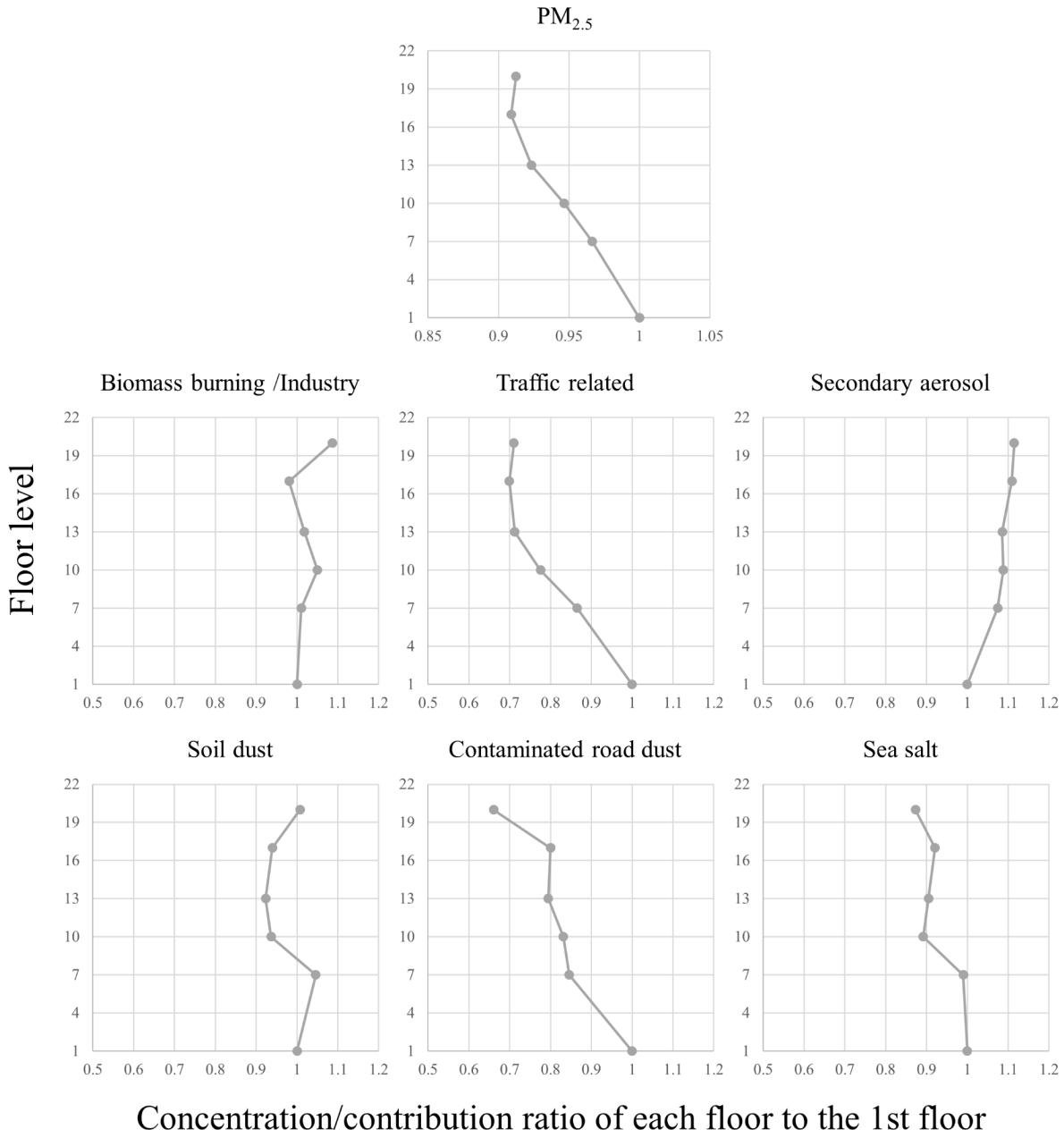

Fig. 3. Vertical distribution patterns of source contribution estimates to $PM_{2.5}$ mass at the sampling site during the study period.

aerosol, the largest contributor to $PM_{2.5}$, slightly increased with height although without any significant difference between floor levels. The increasing trend indicated the partial influence of regional transport (Wu *et al.*, 2015). The other three source factors did not exhibit specific pattern of vertical variation and showed no significant differences in contributions between floor levels. The comparable contributions among floor levels might reveal multiple source origins (Liao *et al.*, 2021). For example, soil dust could originate from local sources and also be transported from distant areas.

Contributions of road traffic emissions significantly declined with height (29.3%–21.4%), which was in conformity with the findings in previous studies (Moeinaddini *et al.*, 2014; Wu *et al.*, 2015; Wang *et al.*, 2016; Liao *et al.*, 2020), and could explain the vertical variation of $PM_{2.5}$ identified in this study. The above results indicated considerable contributions from local ground-level emissions in the study area. Since road traffic emission is known to have a specific temporal pattern, closing windows during rush hour could prevent exposure to high levels of air pollutants. These results

help improve our knowledge about the vertical characteristics of $PM_{2.5}$ sources. It should be noted that long-term exposure patterns to $PM_{2.5}$ warrant further investigation since this study was conducted in a short period of time (19 days within two months).

4 CONCLUSIONS

In this study we explored the vertical characteristics of potential $PM_{2.5}$ sources apportioned by the PMF modeling. In addition to secondary aerosol, road traffic emissions (traffic related and contaminated road dust) represented the second largest contributor to $PM_{2.5}$ during the study period. Contributions of road traffic emissions significantly declined with height, which were similar to the results of previous studies that collected $PM_{2.5}$ samples at three floors from buildings lower than 40 m. In the present study, a broader vertical distribution pattern (six floor-levels) up to 63 m was investigated. The non-significant difference between the 17^{th} and 20^{th} floors suggested that the declining trend was limited at a certain height. With regard to the other source factors, they showed non-significant vertical variation. Consequently, the vertical variation of $PM_{2.5}$ identified in this study could be explained by road traffic emissions. Our findings suggested that enhanced traffic emission control policies could be beneficial in reducing $PM_{2.5}$ exposure for residents living in apartment buildings in metropolitan areas.

ACKNOWLEDGMENTS

This study was supported in part by research grants from the Ministry of Science and Technology of Taiwan (MOST 106-2221-E-002-021-MY3, 109-2221-E-002-057-MY3, and 110-2811-E-002-502-MY3) and the "National Taiwan University Higher Education Sprout Project (NTU-111L8810)" within the framework of the Higher Education Sprout Project by the Ministry of Education (MOE) in Taiwan.

DISCLAIMER

The authors declare that they have no known competing financial interests or personal relationships that could have appeared to influence the work reported in this paper.

REFERENCES

Adachi, K., Tainosho, Y. (2004). Characterization of heavy metal particles embedded in tire dust. Environ. Int. 30, 1009–1017. https://doi.org/10.1016/j.envint.2004.04.004

Adachi, K., Buseck, P.R. (2015). Changes in shape and composition of sea-salt particles upon aging in an urban atmosphere. Atmos. Environ. 100, 1–9. https://doi.org/10.1016/j.atmosenv.2014.10.036

Carnelos, D.A., Portela, S.I., Jobbágy, E.G., Jackson, R.B., Di Bella, C.M., Panario, D., Fagúndez, C., Piñeiro-Guerra, J.M., Grion, L., Piñeiro, G. (2019). A first record of bulk atmospheric deposition patterns of major ions in southern South America. Biogeochemistry 144, 261–271. https://doi.org/10.1007/s10533-019-00584-3

Carrero, J.A., Arrizabalaga, I., Bustamante, J., Goienaga, N., Arana, G., Madariaga, J.M. (2013). Diagnosing the traffic impact on roadside soils through a multianalytical data analysis of the concentration profiles of traffic-related elements. Sci. Total Environ. 458–460, 427–434. https://doi.org/10.1016/j.scitotenv.2013.04.047

Chen, H.L., Li, C.P., Tang, C.S., Lung, S.C.C., Chuang, H.C., Chou, D.W., Chang, L.T. (2020). Risk assessment for people exposed to $PM_{2.5}$ and constituents at different vertical heights in an urban area of Taiwan. Atmosphere 11, 1145. https://doi.org/10.3390/atmos11111145

Cheng, M.T., Horng, C.L., Su, Y.R., Lin, L.K., Lin, Y.C., Chou, C.C.K. (2009). Particulate matter characteristics during agricultural waste burning in Taichung City, Taiwan. J. Hazard. Mater. 165, 187–192. https://doi.org/10.1016/j.jhazmat.2008.09.101

Daher, N., Ruprecht, A., Invernizzi, G., De Marco, C., Miller-Schulze, J., Heo, J.B., Shafer, M.M., Shelton, B.R., Schauer, J.J., Sioutas, C. (2012). Characterization, sources and redox activity of fine and coarse particulate matter in Milan, Italy. Atmos. Environ. 49, 130–141. https://doi.org/10.1016/j.atmosenv.2011.12.011

Dai, Q.L., Bi, X.H., Wu, J.H., Zhang, Y.F., Wang, J., Xu, H., Yao, L., Jiao, L., Feng, Y.C. (2015). Characterization and source identification of heavy metals in ambient PM_{10} and $PM_{2.5}$ in an integrated iron and steel industry zone compared with a background site. Aerosol Air Qual. Res. 15, 875–887. https://doi.org/10.4209/aaqr.2014.09.0226

Ghosh, A., Roy, A., Chatterjee, A., Das, S.K., Ghosh, S.K., Raha, S. (2019). Impact of biomass burning plumes on the size-segregated aerosol chemistry over an urban atmosphere at Indo-Gangetic Plain. Aerosol Air Qual. Res. 19, 163–180. https://doi.org/10.4209/aaqr.2017.12.0590

Gugamsetty, B., Wei, H., Liu, C.N., Awasthi, A., Hsu, S.C., Tsai, C.J., Roam, G.D., Wu, Y.C., Chen, C.F. (2012). Source characterization and apportionment of PM_{10}, $PM_{2.5}$ and $PM_{0.1}$ by using positive matrix factorization. Aerosol Air Qual. Res. 12, 476–491. https://doi.org/10.4209/aaqr.2012.04.0084

Ho, W.Y., Tseng, K.H., Liou, M.L., Chan, C.C., Wang, C.H. (2018). Application of positive matrix factorization in the identification of the sources of $PM_{2.5}$ in Taipei City. Int. J. Environ. Res. Public Health 15, 1305. https://doi.org/10.3390/ijerph15071305

Hopke, P.K. (2016). Review of receptor modeling methods for source apportionment. J. Air Waste Manage. Assoc. 66, 237–259. https://doi.org/10.1080/10962247.2016.1140693

Hopke, P.K., Dai, Q., Li, L., Feng, Y. (2020). Global review of recent source apportionments for airborne particulate matter. Sci. Total Environ. 740, 140091. https://doi.org/10.1016/j.scitotenv.2020.140091

Hsu, C.Y., Chiang, H.C., Chen, M.J., Chuang, C.Y., Tsen, C.M., Fang, G.C., Tsai, Y.I., Chen, N.T., Lin, T.Y., Lin, S.L., Chen, Y.C. (2017). Ambient $PM_{2.5}$ in the residential area near industrial complexes: Spatiotemporal variation, source apportionment, and health impact. Sci. Total Environ. 590, 204–214. https://doi.org/10.1016/j.scitotenv.2017.02.212

Huang, X., Olmez, I., Aras, N.K., Gordon, G.E. (1994). Emissions of trace elements from motor vehicles: Potential marker elements and source composition profile. Atmos. Environ. 28, 1385–1391. https://doi.org/10.1016/1352-2310(94)90201-1

International Agency for Research on Cancer (IARC) (2016). IARC Monographs on the Evaluation of Carcinogenic Risks to Humans: Vol. 109, Outdoor Air Pollution. Lyon, France.

Jin, X.C., Xiao, C.J., Li, J., Huang, D.H., Yuan, G.J., Yao, Y.G., Wang, X.H., Hua, L., Zhang, G.Y., Cao, L., Wang, P.S., Ni, B.F. (2016). Source apportionment of $PM_{2.5}$ in Beijing using positive matrix factorization. J. Radioanal. Nucl. Chem. 307, 2147–2154. https://doi.org/10.1007/s10967-015-4544-0

Jin, Y., Yan, C., Sullivan, A.P., Liu, Y., Wang, X., Dong, H., Chen, S., Zeng, L., Collett, J.J.L., Zheng, M. (2020). Significant contribution of primary sources to water-soluble organic carbon during spring in Beijing, China. Atmosphere 11, 395. https://doi.org/10.3390/atmos11040395

Kim, E., Hopke, P.K., Edgerton, E.S. (2003). Source identification of Atlanta aerosol by positive matrix factorization. J. Air Waste Manage. Assoc. 53, 731–739. https://doi.org/10.1080/10473289.2003.10466209

Kim, K.H., Kabir, E., Kabir, S. (2015). A review on the human health impact of airborne particulate matter. Environ. Int. 74, 136–143. https://doi.org/10.1016/j.envint.2014.10.005

Lane, D.J., Sippula, O., Peräniemi, S., Jokiniemi, J. (2020). Detoxification of wood-combustion ashes containing Cr and Cd by thermal treatment. J. Hazard. Mater. 400, 123315. https://doi.org/10.1016/j.jhazmat.2020.123315

Lee, E., Chan, C.K., Paatero, P. (1999). Application of positive matrix factorization in source apportionment of particulate pollutants in Hong Kong. Atmos. Environ. 33, 3201–3212. https://doi.org/10.1016/S1352-2310(99)00113-2

Liao, H.T., Yau, Y.C., Huang, C.S., Chen, N., Chow, J.C., Watson, J.G., Tsai, S.W., Chou, C.C.K., Wu, C.F. (2017). Source apportionment of urban air pollutants using constrained receptor models with a priori profile information. Environ. Pollut. 227, 323–333. https://doi.org/10.1016/j.envpol.2017.04.071

Liao, H.T., Wu, C.F. (2020). Trajectory-assisted source apportionment of winter-time aerosol using

semi-continuous measurements. Arch. Environ. Contam. Toxicol. 78, 430–438. https://doi.org/10.1007/s00244-020-00714-1

Liao, H.T., Chang, J.C., Tsai, T.T., Tsai, S.W., Chou, C.C.K., Wu, C.F. (2020). Vertical distribution of source apportioned $PM_{2.5}$ using particulate-bound elements and polycyclic aromatic hydrocarbons in an urban area. J. Exposure Sci. Environ. Epidemiol. 30, 659–669. https://doi.org/10.1038/s41370-019-0153-2

Liao, H.T., Lee, C.L., Tsai, W.C., Yu, J.Z., Tsai, S.W., Chou, C.C.K., Wu, C.F. (2021). Source apportionment of urban $PM_{2.5}$ using positive matrix factorization with vertically distributed measurements of trace elements and nonpolar organic compounds. Atmos. Pollut. Res. 12, 200–207. https://doi.org/10.1016/j.apr.2021.03.007

Lu, F., Xu, D.Q., Cheng, Y.B., Dong, S.X., Guo, C., Jiang, X., Zheng, X.Y. (2015). Systematic review and meta-analysis of the adverse health effects of ambient $PM_{2.5}$ and PM_{10} pollution in the Chinese population. Environ. Res. 136, 196–204. https://doi.org/10.1016/j.envres.2014.06.029

Moeinaddini, M., Esmaili Sari, A., Riyahi bakhtiari, A., Chan, A.Y.C., Taghavi, S.M., Hawker, D., Connell, D. (2014). Source apportionment of PAHs and n-alkanes in respirable particles in Tehran, Iran by wind sector and vertical profile. Environ. Sci. Pollut. Res. 21, 7757–7772. https://doi.org/10.1007/s11356-014-2694-1

Norris, G., Duvall, R., Brown, S., Bai, S. (2014). EPA positive matrix factorization (PMF) 5.0 fundamentals and user guide. U.S. Environmental Protection Agency, Washington, DC.

Paatero, P., Tapper, U. (1994). Positive matrix factorization: A non-negative factor model with optimal utilization of error estimates of data values. Environmetrics 5, 111–126. https://doi.org/10.1002/env.3170050203

Pandolfi, M., Gonzalez-Castanedo, Y., Alastuey, A., de la Rosa, J.D., Mantilla, E., de la Campa, A.S., Querol, X., Pey, J., Amato, F., Moreno, T. (2011). Source apportionment of PM_{10} and $PM_{2.5}$ at multiple sites in the strait of Gibraltar by PMF: impact of shipping emissions. Environ. Sci. Pollut. Res. Int. 18, 260–269. https://doi.org/10.1007/s11356-010-0373-4

Pio, C., Mirante, F., Oliveira, C., Matos, M., Caseiro, A., Oliveira, C., Querol, X., Alves, C., Martins, N., Cerqueira, M., Camões, F., Silva, H., Plana, F. (2013). Size-segregated chemical composition of aerosol emissions in an urban road tunnel in Portugal. Atmos. Environ. 71, 15–25. https://doi.org/10.1016/j.atmosenv.2013.01.037

Ponco Wardoyo, A.Y., Dharmawan, H.A. (2019). Developing reheated motorcycle exhaust for $PM_{2.5}$ emission. Int. J. GEOMATE 16, 109–116. https://doi.org/10.21660/2019.54.8180

Qi, L., Chen, M.D., Ge, X.L., Zhang, Y.F., Guo, B.F. (2016). Seasonal variations and sources of 17 aerosol metal elements in suburban Nanjing, China. Atmosphere 7, 21. https://doi.org/10.3390/atmos7120153

Schneider, I.L., Teixeira, E.C., Dotto, G.L., Pinto, D., Yang, C.X., Silva, L.F.O. (2022). Geochemical study of submicron particulate matter (PM_1) in a metropolitan area. Geosci. Front. 13, 101130. https://doi.org/10.1016/j.gsf.2020.12.011

Silva, L.F.O., Schneider, I.L., Artaxo, P., Núñez-Blanco, Y., Pinto, D., Flores, É.M.M., Gómez-Plata, L., Ramírez, O., Dotto, G.L. (2022). Particulate matter geochemistry of a highly industrialized region in the Caribbean: Basis for future toxicological studies. Geosci. Front. 13, 101115. https://doi.org/10.1016/j.gsf.2020.11.012

Song, C.H., Ma, Y., Orsini, D., Kim, Y.P., Weber, R.J. (2005). An investigation into the ionic chemical composition and mixing state of biomass burning particles recorded during TRACE-P P3B Flight#10. J. Atmos. Chem. 51, 43–64. https://doi.org/10.1007/s10874-005-5727-9

Sudheer, A.K., Rengarajan, R., Deka, D., Bhushan, R., Singh, S.K., Aslam, M.Y. (2014). Diurnal and seasonal characteristics of aerosol ionic constituents over an urban location in Western India: Secondary aerosol formation and meteorological influence. Aerosol Air Qual. Res. 14, 1701–1713. https://doi.org/10.4209/aaqr.2013.09.0288

Taiwo, A.M., Beddows, D.C.S., Shi, Z.B., Harrison, R.M. (2014). Mass and number size distributions of particulate matter components: Comparison of an industrial site and an urban background site. Sci. Total Environ. 475, 29–38. https://doi.org/10.1016/j.scitotenv.2013.12.076

Tang, I.N., Tridico, A.C., Fung, K.H. (1997). Thermodynamic and optical properties of sea salt aerosols. J. Geophys. Res. 102, 23269–23275. https://doi.org/10.1029/97JD01806

Thepnuan, D., Chantara, S., Lee, C.T., Lin, N.H., Tsai, Y.I. (2019). Molecular markers for biomass

burning associated with the characterization of $PM_{2.5}$ and component sources during dry season haze episodes in Upper South East Asia. Sci. Total Environ. 658, 708–722. https://doi.org/10.1016/j.scitotenv.2018.12.201

Todorović, M.N., Radenković, M.B., Onjia, A.E., Ignjatović, L.M. (2020). Characterization of $PM_{2.5}$ sources in a Belgrade suburban area: A multi-scale receptor-oriented approach. Environ. Sci. Pollut. Res. 27, 41717–41730. https://doi.org/10.1007/s11356-020-10129-z

United Nations (2018). World Urbanization Prospects: The 2018 Revision, Online Edition.

Wang, J., Zhou, M., Liu, B.S., Wu, J.H., Peng, X., Zhang, Y.F., Han, S.Q., Feng, Y.C., Zhu, T. (2016). Characterization and source apportionment of size-segregated atmospheric particulate matter collected at ground level and from the urban canopy in Tianjin. Environ. Pollut. 219, 982–992. https://doi.org/10.1016/j.envpol.2016.10.069

Wang, Y., Plewa, M.J., Mukherjee, U.K., Verma, V. (2018). Assessing the cytotoxicity of ambient particulate matter (PM) using Chinese hamster ovary (CHO) cells and its relationship with the PM chemical composition and oxidative potential. Atmos. Environ. 179, 132–141. https://doi.org/10.1016/j.atmosenv.2018.02.025

Wen, J., Shi, G., Tian, Y., Chen, G., Liu, J., Huang-Fu, Y., Ivey, C.E., Feng, Y. (2018). Source contributions to water-soluble organic carbon and water-insoluble organic carbon in $PM_{2.5}$ during Spring Festival, heating and non-heating seasons. Ecotoxicol. Environ. Saf. 164, 172–180. https://doi.org/10.1016/j.ecoenv.2018.08.002

Wimolwattanapun, W., Hopke, P.K., Pongkiatkul, P. (2011). Source apportionment and potential source locations of $PM_{2.5}$ and $PM_{2.5\text{-}10}$ at residential sites in metropolitan Bangkok. Atmos. Pollut. Res. 2, 172–181. https://doi.org/10.5094/APR.2011.022

World Health Organization (WHO) (2021). World health statistics 2021: Monitoring health for the SDGs, sustainable development goals. World Health Organization, Geneva.

Wu, H., Zhang, Y.F., Han, S.Q., Wu, J.H., Bi, X.H., Shi, G.L., Wang, J., Yao, Q., Cai, Z.Y., Liu, J.L., Feng, Y.C. (2015). Vertical characteristics of $PM_{2.5}$ during the heating season in Tianjin, China. Sci. Total Environ. 523, 152–160. https://doi.org/10.1016/j.scitotenv.2015.03.119

Xie, M., Coons, T.L., Hemann, J.G., Dutton, S.J., Milford, J.B., Peel, J.L., Miller, S.L., Kim, S.Y., Vedal, S., Sheppard, L., Hannigan, M.P. (2012). Intra-urban spatial variability and uncertainty assessment of $PM_{2.5}$ sources based on carbonaceous species. Atmos. Environ. 60, 305–315. https://doi.org/10.1016/j.atmosenv.2012.06.036

Yin, S., Huang, Z., Zheng, J., Huang, X., Chen, D., Tan, H. (2018). Characteristics of inorganic aerosol formation over ammonia-poor and ammonia-rich areas in the Pearl River Delta region, China. Atmos. Environ. 177, 120–131. https://doi.org/10.1016/j.atmosenv.2018.01.005

Zauli Sajani, S., Marchesi, S., Trentini, A., Bacco, D., Zigola, C., Rovelli, S., Ricciardelli, I., Maccone, C., Lauriola, P., Cavallo, D.M., Poluzzi, V., Cattaneo, A., Harrison, R.M. (2018). Vertical variation of $PM_{2.5}$ mass and chemical composition, particle size distribution, NO_2, and BTEX at a high rise building. Environ. Pollut. 235, 339–349. https://doi.org/10.1016/j.envpol.2017.12.090

Zhang, D., Pan, X., Lee, D.J. (2014). Potentially harmful metals and metalloids in the urban street dusts of Taipei City. J. Taiwan Inst. Chem. Eng. 45, 1727–1732. https://doi.org/10.1016/j.jtice.2014.01.003